UCRL-TR-212726

LAWRENCE
LIVERMORE
NATIONAL
LABORATORY

An Integral Method for Determining Induced Voltage in Time-Varying Wire Inductors

B. Fasenfest, D. White, J. Rockway

June 6, 2005

This work was performed under the auspices of the U.S. Department of Energy by University of California, Lawrence Livermore National Laboratory under Contract W-7405-Eng-48.

An Integral Method for Determining Induced Voltage in Time-Varying Wire Inductors

Benjamin Fasenfest

Dan White

John Rockway

March 18, 2005

I. Introduction

This report documents the creation of software tools to model time-varying wire inductors. The class of inductors studied consists of arbitrary wire shapes in non-magnetic material. When the wire structures are deformed, the inductance changes, and a voltage is induced. This voltage is of interest, for instance when the inductor is used to measure or sense a shockwave. An integral technique, which only requires integrating over the wire segments, is used to find the inductance at each time step, with backwards-difference approximations being used on successive time steps to determine the voltage. This method allows for arbitrary time-varying wire structures. It was tested for several canonical problems and used to model a double helix solenoid compressed by a shockwave.

II. Formulation

One method of calculating inductance is from stored energy. For a single conductor, inductance is related to stored energy by

$$L = \frac{2W_m}{I^2}, \qquad (1)$$

Where L is the inductance, I is the current, and W_m is the stored magnetic energy. Stored energy can be written either as an integral of the magnetic flux density over all space,

$$W_m = \frac{1}{2}\int_V \frac{B^2}{\mu} dV \qquad (2)$$

or as an integral over only the current-carrying regions,

$$W_m = \frac{1}{2}\int_V \boldsymbol{A} \bullet \boldsymbol{J} dV , \qquad (3)$$

where **A** is the magnetic vector potential found from the current density **J** by

$$\boldsymbol{A}(\boldsymbol{r}) = \frac{\mu_0}{4\pi}\int_{V'} \frac{\boldsymbol{J}(\boldsymbol{r}')}{|\boldsymbol{r} - \boldsymbol{r}'|} dV' . \qquad (4)$$

To make use of equation (4), the actual wire inductor is represented by many connected straight wire segments. On a short wire segment at DC, the current will be evenly distributed throughout the cross section of the wire, and can be assumed to flow straight down the wire. This leads to a current density vector on the nth segment of

$$\boldsymbol{J}_n = \frac{\hat{\boldsymbol{l}}_n}{\pi a^2} \qquad (5)$$

where a is the wire radius and $\hat{\boldsymbol{l}}_n$ is the unit vector along the wire. For mutual inductance between wire segments, it is assumed that the wire radius is less than the separation between wires so that current-carrying filaments can replace both wires. This replacement is common in inductance calculations [1,2], and allows the integral in equation (4) to be reduced to

$$\boldsymbol{A}(\boldsymbol{r}) = \frac{\mu_0}{4\pi}\int_{l'} \frac{\hat{\boldsymbol{l}}'}{|\boldsymbol{r} - \boldsymbol{r}'|} dl' , \qquad (6)$$

leading to a mutual inductance of

$$L_{mn} = \frac{\mu_0}{4\pi}\int_{l}\int_{l'}\frac{\hat{\boldsymbol{l}}_{\boldsymbol{m}} \bullet \hat{\boldsymbol{l}}'_{\boldsymbol{n}}}{\left|\mathbf{r} - \mathbf{r}'\right|}dl'dl \qquad (7).$$

For the self-induction of a wire segment, the approximate result

$$L_{mm} \approx \frac{\mu_0 l_m}{2\pi}\left[\ln\left(\frac{2l_m}{a}\right) - 0.75\right] = 2\times10^{-7} l_m \left[\ln\left(\frac{2l_m}{a}\right) - 0.75\right] \qquad (8)$$

found in [3] is used. To find the total inductance of the wire structure, the self-inductance for every wire and the mutual inductance for every pair of wires is computed and summed.

Resistance for a wire segment can be found from the equation

$$R_m = \frac{\rho_m l_m}{\pi a^2} \qquad (9)$$

where ρ_m is the electrical resistivity of the wire m. The total resistance is simply the sum of the resistance for each wire segment.

The voltage across the inductor terminals will be given by

$$V(t) = \frac{dL}{dt}I + R(t)I\ . \qquad (10)$$

If a simple backwards-difference approximation is used for the derivative, equation (10) becomes

$$V(t_n) = \frac{L_n - L_{n-1}}{\Delta t}I + R\left(t_n\right)I\ . \qquad (11)$$

With an order $O\left(\Delta t^2\right)$ accurate backwards-difference approximation, equation (10) becomes

$$V(t_n) = \frac{3L_n - 4L_{n-1} + L_{n-1}}{2\Delta t}I + R\left(t_n\right)I\ . \qquad (12)$$

Note that equation (10) assumes a constant current through the inductor.

III. Software Validation

Two main drivers were created to implement the formulation. These test drivers rely on the BEMSTER boundary-element libraries for integration rules, element geometry descriptions, and Green's functions. The first driver, ComputeLFromWire, reads in a wire mesh in .jfg format (exported from MESHANTS) and computes the total inductance. It is capable of running parametric sweeps on wire radius as well as on the number of integration points used. Since the same quadrature rules are used for the source and testing integrations in equation (7) and there are no anisotropic materials, the mutual inductance $L_{mn} = L_{nm}$, and only half of the interactions need to be computed.

To test the method, a circular wire loop with a loop radius R 1 m and a wire radius r of 1 cm was simulated. The exact solution for the self-inductance of a circular wire loop is given by

$$L = 4\pi R\left(\ln\left(\frac{8R}{r}\right)-\frac{7}{4}\right)\times 10^{-7}\ H,\ [4] \tag{13}$$

or 6.201e-6 for this particular loop. The wire loop was meshed with different numbers of wire segments using MESHANTS, and the inductance was computed with different orders of quadrature rules. The results, graphed in Figure 1, show that the error in the computed solution decrease as the number of segments increases, which is unsurprising. However, it also shows that as the number of segments increases, higher orders of integration quadrature rules are necessary to realize the full accuracy of the geometry discritization. This is likely because as the number of elements increases, adjacent wire segments are getting closer together relative to their length. This ratio of wire segment length to separation requires higher order quadratures to correctly compute the integrals. Although only the "near" segment interactions require this increased quadrature accuracy, for simplicity, all interactions use the same quadrature rule.

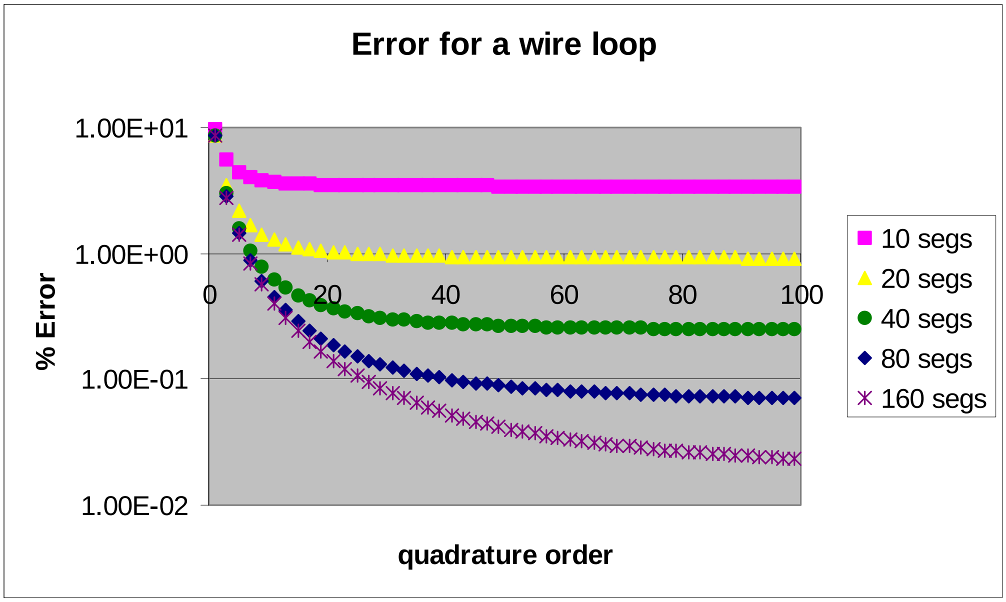

Figure 1. Error in the computed inductance for a wire loop.

Based on the results from Figure 1, 19th order quadrature rules seem an adequate choice for 1 % error in inductance; for every mesh density that could result in less than 1 % error, the error was below that point by 19th order quadrature. However, this increase in quadrature order does increase run time significantly. The cost of evaluating the inductance scales at approximately the square of the number of integration quadrature points times the square of the number of wire segments. This relation can be seen from the run times for the loop, shown in Figure 2. Because of accuracy issues with the timing routine used, the time reported for simulations taking of less than a hundredth of a second are not very accurate. However, the scaling of run time with the number of segments and the quadrature order can still be seen.

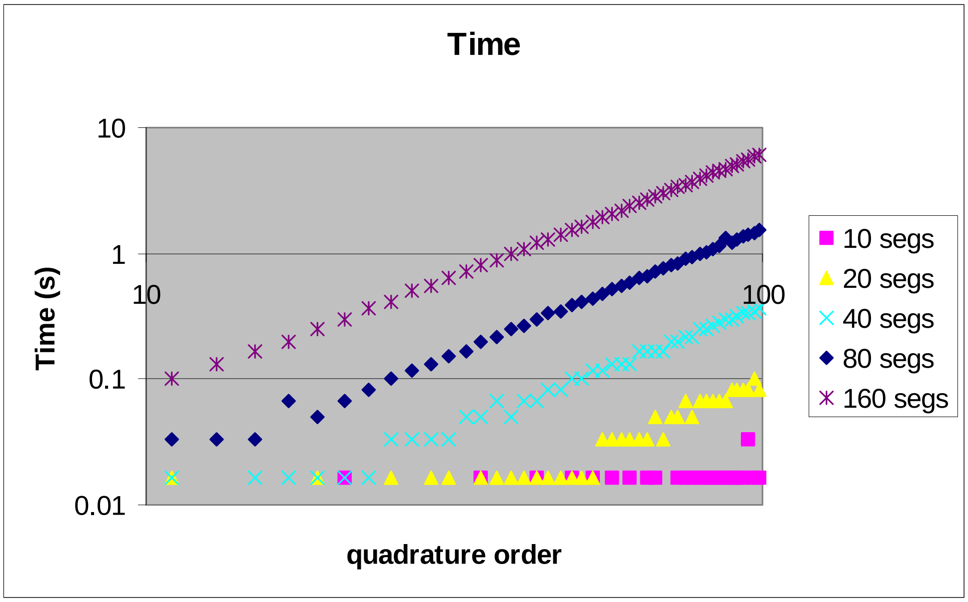

Figure 2. CPU time required to calculate the inductance of a circular wire loop.

The second driver, LfromChangingWire, removes the need for an externally generated mesh. Instead, the user enters in the start and stop coordinates of the inductor in cylindrical coordinates and a description of how the inductor varies with time. From this information, the program automatically generates a mesh of the inductor for every time step and computes the induced voltage as a function of time. Equation (11) is used to find the voltage for the first time step, and equation (12) is used for all following time steps.

The test loop used had a starting radius R of 1 m, an ending radius of 0.1 m, a constant wire radius of 1 cm. The loop was assumed to take 50 seconds to transition from the larger to smaller radius. The derivative of inductance with respect to time for a wire loop can be found from (13) as

$$\frac{dL}{dt} = \frac{dL}{dR}\frac{dR}{dt} = 4\pi\left(\ln\left(\frac{8R}{r}\right) - \frac{3}{4}\right)\times 10^{-7}\frac{dR}{dt}. \tag{14}$$

For the loop tested, $\frac{dR}{dt} = 0.018$. The loop was simulated using 80 wire segments and 19th order integration rules. Figure 3 compares the analytic and simulated results for induced voltage when a time step of 0.5 seconds is chosen. Figure 4 shows the simulation re-run with a time step of 0.125 seconds. It can be seen that the results are very good when the time step is chosen small enough. The relationship between error and time step is plotted in Figure 5. It can be seen from the plot that time step choice is an important factor in determining accuracy.

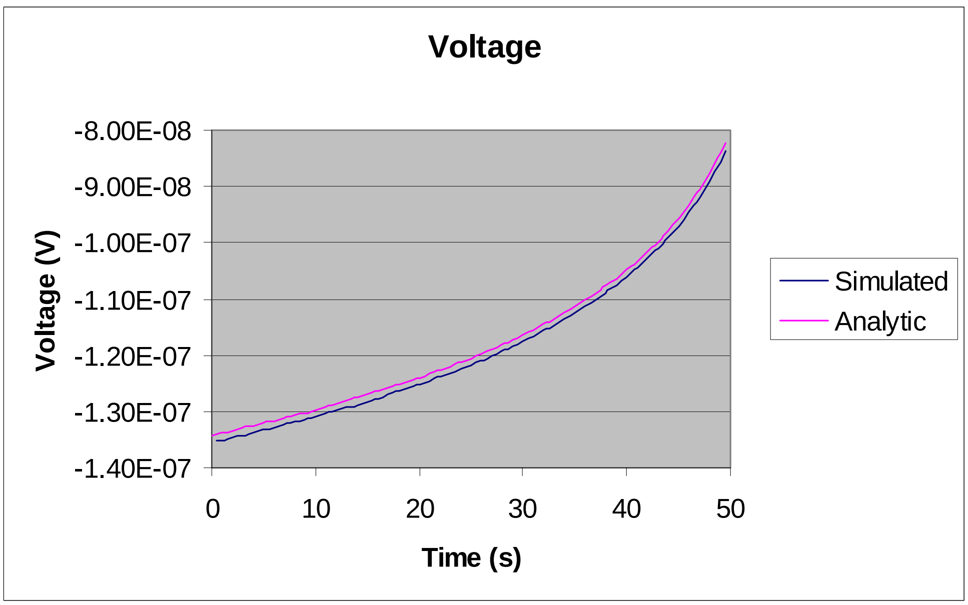

Figure 3. Analytic and simulated results for the induced voltage on a changing wire loop with time step 0.5 seconds.

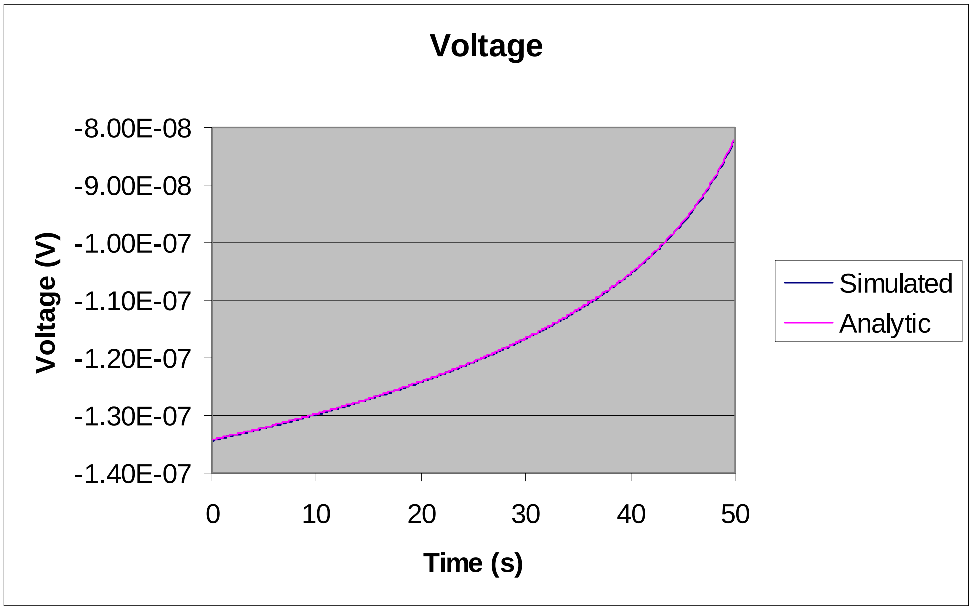

Figure 4. Analytic and simulated results for the induced voltage on a changing wire loop with time step 0.125 seconds.

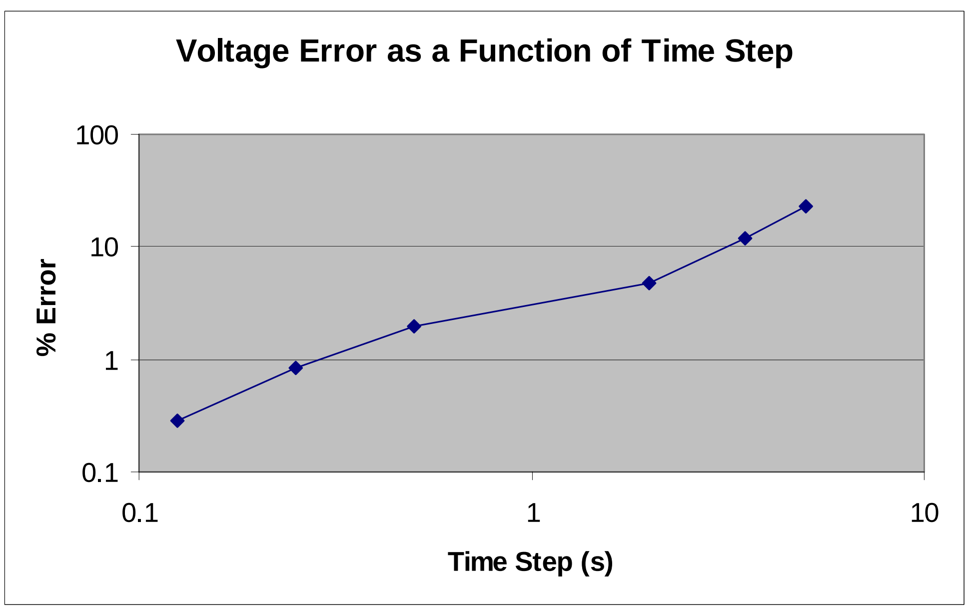

Figure 5. Error in the induced voltage as a function of time step.

IV. Double Helix Results

A modified version of LfromChangingWire was created to model the problem of a double helix inductor compressed by a shockwave. The double helix cross section is shown below in Figure 6. Several parameters are necessary to specify the exact shape of the helix: R1 and R2, the inner and outer radii, N1 and N2, the number of turns in the inner and outer windings, H, the height of the inner winding, S, the offset between the tops of the inner and outer windings, and F, the fraction of a turn used to connect the inner and outer windings. Since S is the offset from the top of the inner winding to the top of the outer winding, it will be negative when the outer winding is closer to the terminals than the inner winding, as shown in Figure 6. F, the fraction of a turn used to connect the inner and outer windings, can be chosen as 0.5 to take a half-turn to go from the inner to outer winding.

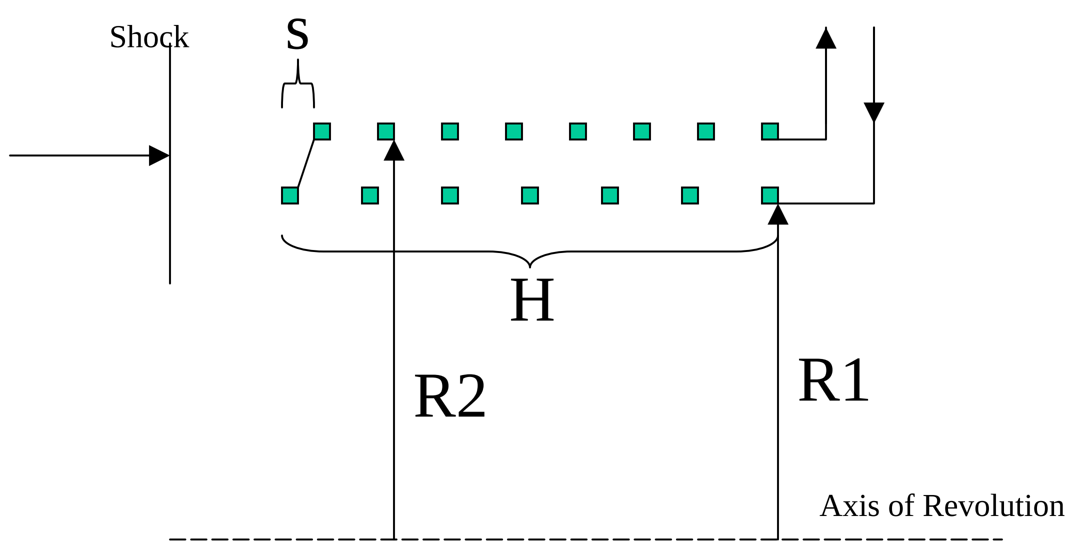

Figure 6. The rotational cross-section of the double helix inductor.

In addition to the initial dimensions of the inductor, several more parameters are needed to describe what happens after the shockwave wavefront has encountered the inductor. The compression ratio, C, describes how much the parts of the inductor that are inside the shockwave have compressed along the length of the helix. The compression algorithm assumes that all of the wire segments behind the wavefront are compressed by the factor C. However, this is not quite a complete description of what would really happen. As the shockwave compressed the helix in Z, it would also slightly expand its radius. However, this expansion is not currently modeled, although it could be added later. The shockwave velocity and the resistance of the wire before and after being heated by the shockwave also need to be specified. Currently, all these parameters are read in from a simple user-generated text file.

At the simulation's completion, two output files are created. One contains a table with the inductance, voltage, and wavefront position for every time step, as well as the CPU time taken to complete the simulation. The second contains the nodes of the wire segments at every time step, which can be used to examine how the shockwave compresses the helix. A simple Matlab script was created to read this file and produce movies or still images of the helix.

A double helix using the parameters in Table 1 was simulated with different numbers of segments. Figures 7 and 8 show the helix in various stages of compression, with the shockwave wavefront shown in red.

Table 1: Parameters for the test helix

R1	1 cm
R2	1.2 cm
N1	5 Turns
N2	5 Turns
H	1 cm
F	0.5 Turns
S	0 cm
C	0.333
Shock Velocity	2000 m/s
Delta T	5.00E-08
Wire Radius	0.1 mm
Resistivity	0

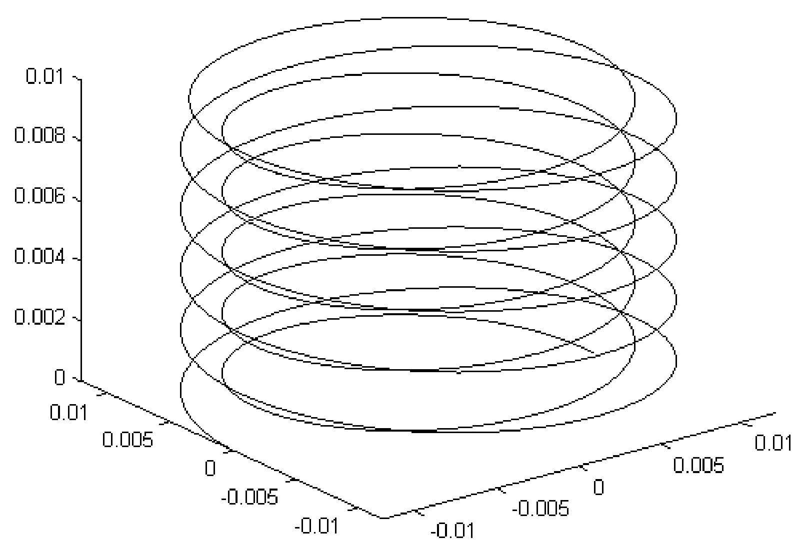

Figure 7. The double helix inductor before the shockwave hits it.

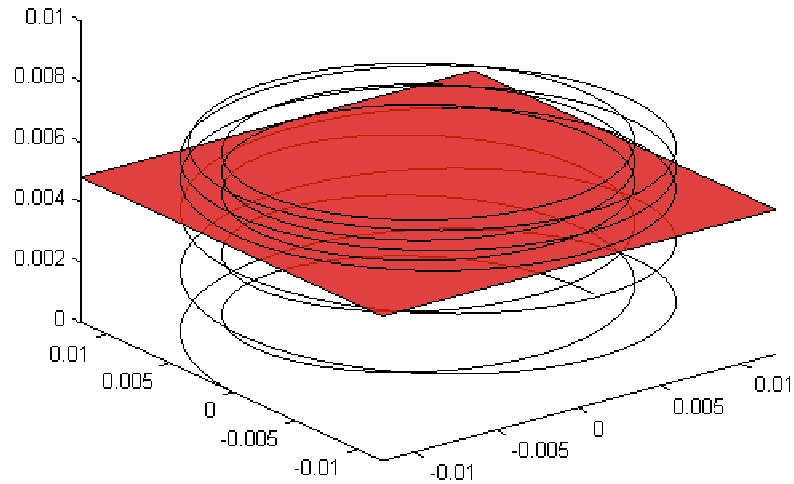

Figure 8. The double helix when the shockwave wavefront (shown in red) has progressed halfway down the original height of the inductor. Note that the portion of the helix that has been hit by the shockwave is compressed to 0.333 times the spacing between turns.

The results for inductance as a function of time and number of wire segments used are shown in Figure 9. The voltage is shown in Figure 10. From these figures, it can be seen that 250 segments adequately resolves the helix. For 250 segments, the entire simulation takes only 17 seconds to complete. With a finer mesh of 1000 segments, the simulation takes 260 seconds. The expectation for this simulation was that if a current of 5-10 A were used, the result would be a few volts. The maximum induced voltage in Figure 8 multiplied by 10 A gives 2.7 V, around what was expected.

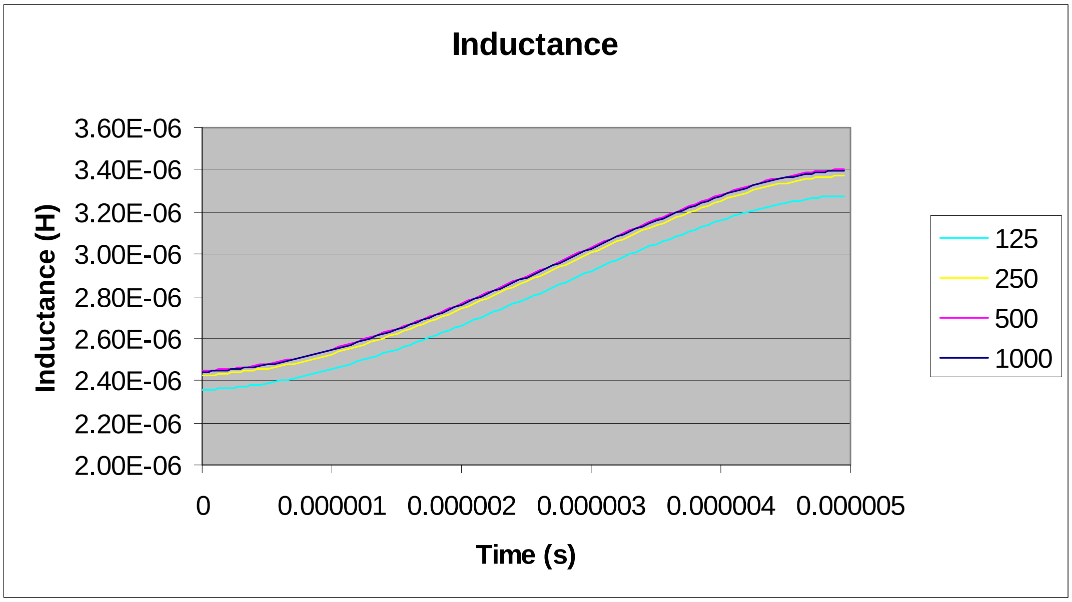

Figure 9. Inductance of a double helix as a function of time and number of wire segments used.

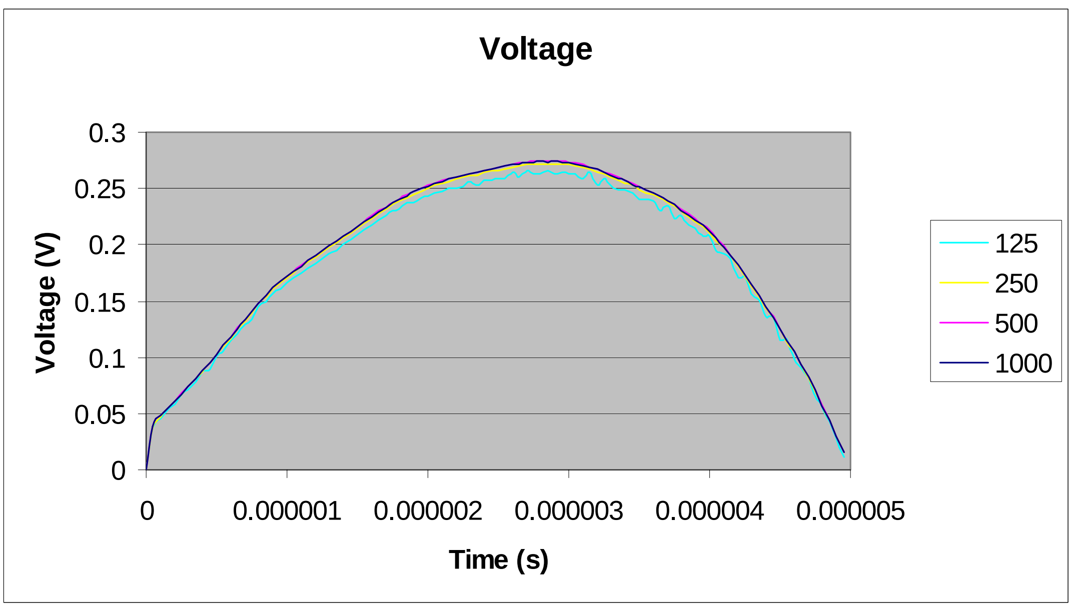

Figure 10. Voltage induced by a double helix as a function of time and number of wire segments used.

V. Future Work

There are still several areas for improvement on the current code. Because the time needed for the inductance calculation at each time step is proportional to the number of elements squared, simulating very large meshes would be very time consuming. These large meshes would be necessary if the number of turns in the helix increased. To combat this increased computational cost, a fast QR decomposition method could be used to accelerate the computation of L at each time step. This method has been used on electrostatic problems and should apply easily to magnetostatics. It has the potential to reduce the cost from $O\left(N^2\right)$ to $O\left(N \log N\right)$. The BEMSTER libraries already contain some basic QR algorithms, which could be extended and further developed for this problem.

A more accurate model of the behavior of the double helix in a shockwave might be necessary for increased accuracy. For instance, the expansion in radius of the inductor after it has been hit by the shockwave could be incorporated into the model. Using the BEMSTER libraries, the magnetic field could be computed at any points in space, such as those needed for plots of the H field. These plots could show how the magnetic field changed as the inductor compressed, and could lead to a greater understanding of the problem. In addition, the magnetic fields could be integrated over all space using equation (2) as an alternate method of computing the inductance of the helix.

VI. Conclusion

A method for calculating the voltage induced by a time-varying inductor was derived based on the integration of the magnetic vector potential. The method was tested against analytic results and shown to be accurate if the time step, number of wire segments, and order of the integration rules was chosen appropriately. The code was then applied to a double helix inductor compressed by a shockwave.

VII. References

[1] Z. Luo and N. A. Demerdash, "The Analysis of the Magnetostatic Fields Surrounding a Twisted-Pair Transmission Line Using Integral Methods," *IEEE Transactions on Magnetics,* September 1992, pp. 2244-2246.

[2] M. Kamon, M.J. Tsuk, J. White, "FastHenry: A Multipole-Accelerated 3-D Inductance Extraction Program," *IEEE Transactions on Microwave Theory and Techniques,* September 1994, pp. 1750-1758.

[3] F. W. Grover, *Inductance Calculations: Working Formulas and Tables,* Dover Publications, Inc., New York, 1946.

[4] "Self Inductance," *http://home.san.rr.com/bushnell/self_inductance.htm,* accessed March 18, 2005.